Engineering Failure Analysis 48 (2015) 166–173

Contents lists available at ScienceDirect

Engineering Failure Analysis

journal homepage: www.elsevier.com/locate/engfailanal

Residual harmfulness of a defect after repairing by a composite patch

T. Nateche [a,b], M. Hadj Meliani [b,c], Shafique M.A. Khan [d], Y.G. Matvienko [e], Nesar Merah [d], G. Pluvinage [c,*]

[a] Maritime Department, USTMB University, Oran, Algeria
[b] LPTPM, Faculty of Technology, Hassiba Benbouali University of Chlef, 02000 Chlef, Algeria
[c] LaBPS–ENIM, University de Lorraine, Metz 57045, France
[d] Department of Mechanical Engineering, King Fahd University of Petroleum and Minerals, Dhahran 31261, Saudi Arabia
[e] Mechanical Engineering Research, Academy of Sciences,101990 Moscow, Russia

ARTICLE INFO

Article history:
Received 1 September 2014
Accepted 18 November 2014
Available online 28 November 2014

Keywords:
Defect repairing
Patch
Residual harmfulness

ABSTRACT

The harmfulness of a defect in a CT specimen made in an API 5L X52 steel pipe is evaluated after being repaired with a composite patch. Due to the fact that the presence of a composite patch improves the fracture resistance but also modifies the constraint, a two-parameter fracture approach is used. More precisely, the stress field at the tip of a notch-like defect repaired by a boron/epoxy bonded composite patch is evaluated by the notch stress intensity factor K_ρ and the effective *T*-stress T_{ef} as constraint parameter. An assessment point of coordinates $[T_{ef}–K_\rho]$ is reported in the Fracture Toughness–Constraint Diagram (FTCD). A line from origin O and passing through this assessment point intercepts the Failure Material Master Curve. This procedure allows us to determine a patch repairing index which is a measure of the residual harmfulness of a crack-like defect after repair. The repair with a composite patch reduces significantly the defect's severity and increases the service life.

1. Introduction

Global energy demands continue to increase with the rapid development of the global economy. The transportation of oil and gas by pipelines is the safest and most economical means for companies transporting hydrocarbons. To increase the profitability of a pipeline, the flow rate is often increased by increasing the service pressure and using larger diameter pipes. Therefore, the performance of pipes must be improved by enhancing their mechanical and chemical characteristics.

The current pipeline networks employ various grades of steel [1], with Grade B, X52 and X60 comprising about 70% of these networks. Pipeline networks are often subjected to damage inducing leak or failure. Recent studies [2] show that more than 50% of failures are caused by external interference.

For many years, the only possible solution to repair damaged pipes was complete replacement or replacement of a section with new pipes. These procedures generally cause costly production losses. Moreover, hot works are forbidden during the replacement in dangerous zones. In addition, metallurgical mismatch and residual stresses caused by welding add disadvantages to this complicated and costly solution. To avoid replacing the damaged structure, for both economic and technical reasons, a recent solution is to use a composite patch over the damaged area with an adhesive [3–5].

* Corresponding author.

http://dx.doi.org/10.1016/j.engfailanal.2014.11.010
1350-6307/

In this paper, the harmfulness of a defect is evaluated after being repaired with a composite patch. Due to the fact that the presence of a composite patch improves the fracture resistance but also modifies the constraint, a two-parameter fracture approach is used. More precisely the stress field at the tip of a notch-like defect repaired by a boron/epoxy bonded composite patch is evaluated by the applied notch stress intensity factor K_ρ and the effective T-stress T_{ef} as constraint parameter. An assessment point of coordinates $[T_{ef}–K_\rho]$ is reported in the Fracture Toughness–Constraint Diagram (FTCD). A line from origin O and passing through this assessment point intercepts the Failure Material Master Curve. This procedure allows the determination of a patch repairing index which is a measure of the residual severity of a crack-like defect after repair. The notch stress intensity factor is determined by the Volumetric Method (VM) [6] and the constraint by the Stress Difference Method (SDM) [7].

This study has been made on CT specimens made in pipe steel X 52 and covered with 2 types of epoxy boron composite patch.

2. Material and specimen

Compact Tension (CT) specimens with mechanical notches of different lengths are prepared using pipe steel X52. Several relative notch lengths a/W are studied: 0.2, 0.3, 0.4, 0.5 and 0.6, where a is the notch length and W the specimen width. The CT specimens have the following dimensions: length = 63.8 mm, width = 61 mm, thickness = 5.84 mm and notch radius ρ = 0.25 mm. The width of the repair patches is 18 mm and thickness is 2 mm. Two different lengths of repair patch are used: type III: the length of patch is the same as the length of the CT specimen (63.8 mm), and type II: the length of patch is half the length of the CT specimen (32.9 mm). The thickness of the adhesive in all cases is 0.3 mm. The material is assumed to remain elastic until fracture and the elastic constants of the materials are given in Table 1. The steel and the adhesive are considered as isotropic while the composite patch is modelled as orthotropic (see Fig. 1).

3. Stress distribution at notch tip using FEM method

The stress distribution at the notch tip of specimens with and without patches is determined by the 3D Finite Element method by means of Abaqus/CAE™. The solid model is meshed using linear 8-noded hexahedral elements with a total of

Table 1
Mechanical properties (CT specimen, patch and adhesive).

Properties	API 5L X52	Boron/epoxy	Adhesive
E_1 (GPa)	210	200	2.723
E_2 (GPa)		25	
E_3 (GPa)		25	
ν_{12}	0.33	0.21	0.294
ν_{13}		0.21	
ν_{23}		0.21	
G_{12} (GPa)		7.2	
G_{13} (GPa)		5.5	
G_{23} (GPa)		5.5	

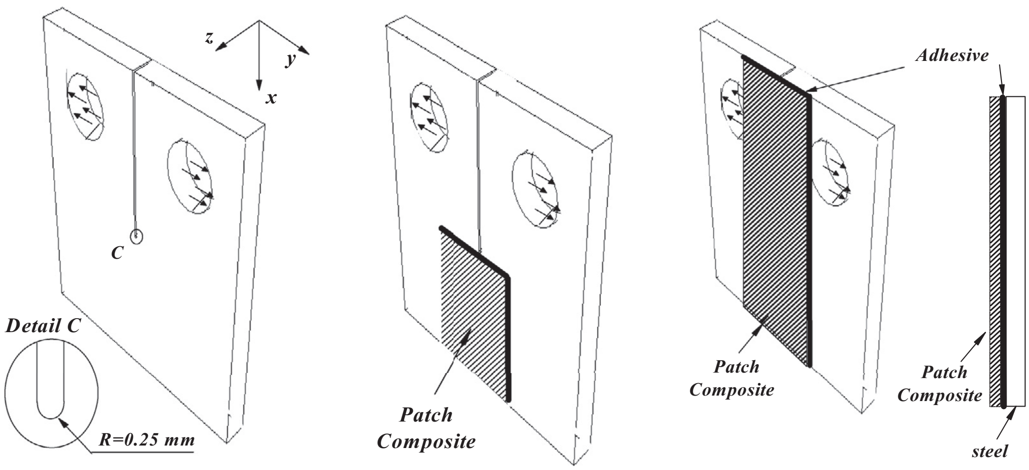

Fig. 1. Types of studied specimen.

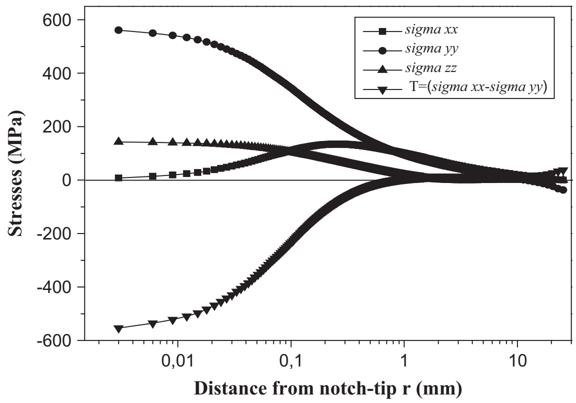

Fig. 2. Stress distribution σ_{yy}, σ_{xx} and σ_{zz} relative to a CT specimen without patch for a 1000 N load and at mid thickness.

Table 2
Failure load according to relative notch depth a/W of CT specimens [8].

Relative notch depth a/W	Failure load in $[N]$
0.2	32,098
0.3	25,270
0.4	18,988
0.5	12,570
0.6	5878

192,016 elements, including 119,152 in the CT specimen and 72,864 elements in the composite repair patch and the adhesive layer. A finer mesh is used at the notch tip (mesh size of about 1 μm). Fig. 2 shows the mesh used in this study. The structure is symmetrical about its centre line, therefore only half of the CT specimen is modelled. Therefore, symmetric boundary conditions in the $x-z$ plane of the specimen were applied (the displacement in the y direction is thus prevented) for the CT specimen, repair patch and adhesive layer. The applied load is modelled as a pressure on the inner surfaces of the pinholes of the CT specimen.

The study was conducted in 2 steps:

(a) The specimens with and without patches and with different relative notch depths a/W are subjected to the same tensile load of 1000 N in the direction normal to the notch direction.
(b) The specimens with and without patches and with different relative notch depths a/W are subjected to the failure tensile load in the direction normal to the notch direction. These failure loads are different for the various a/W ratios. They are given in Ref. [8] and are reported in Table 2.

Fig. 2 shows the distribution of the σ_{yy}, σ_{xx} and σ_{zz} stresses. The opening stress σ_{yy} is normal to notch direction. This distribution is relative to a CT specimen without a patch for a 1000 N load and at mid thickness. We note that the stress distribution has its maximum at the notch tip.

4. Determination of notch stress intensity factor

Determination of the notch stress intensity factor for a notch-like defect is made using the Volumetric Method. The Volumetric Method (VM) [6] is a local fracture criterion which assumes that the fracture process requires a certain volume. This volume is assumed as a cylindrical volume with effective distance as its diameter. The physical meaning of this fracture process volume is "the high stressed region" where the necessary fracture energy release rate is stored. The difficulty is to find the limit of this "high stressed region". This limit is a priori not a material constant but depends on loading mode, structure geometry and load level. The size of the fracture process reduced to the effective distance X_{ef} according to the above-mentioned assumptions is obtained by examination of the stress distribution.

The bi-logarithmic elastic–plastic stress distribution (Fig. 3) along the ligament exhibits three distinct zones which can be easily distinguished. The elastic–plastic stress primarily increases and it attains a peak value (zone I) then it gradually drops to the elastic–plastic regime (zone II). Zone III represents linear behaviour in the bi-logarithmic diagram. It has been proved by examination of fracture initiation sites that the effective distance corresponds to the beginning of zone III, which is in fact an inflexion point on this bi-logarithmic stress distribution. A graphical method based on the relative stress gradient χ associates the effective distance with the minimum of χ. The relative stress gradient is given by:

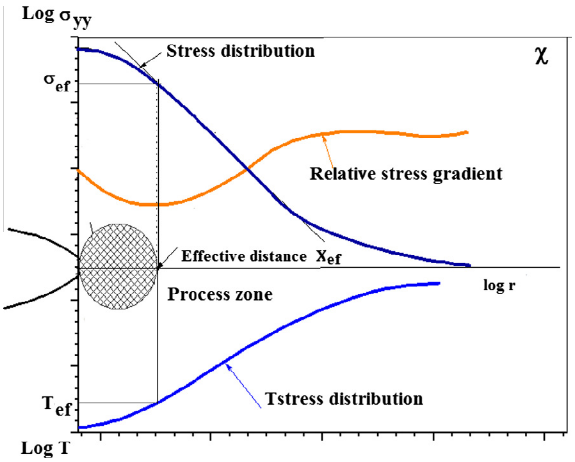

Fig. 3. Schematic stress distribution along notch ligament and notch stress intensity concept.

$$\chi(r) = \frac{1}{\sigma_{yy}(r)} \frac{\partial \sigma_{yy}(r)}{\partial r} \tag{1}$$

where $\chi(r)$ and $\sigma_{yy}(r)$ are the relative stress gradient and maximum principal stress or opening stress, respectively.

The effective stress for fracture σ_{ef} is then considered to be the average value of the stress distribution over the effective distance. However, stresses are multiplied by a weight function in order to take into account the stress gradient due to geometry and loading mode and acting distance r. The stress distribution is then given by:

$$\sigma_{ef} = \frac{1}{X_{ef}} \int_0^{X_{ef}} \sigma_{yy}(r) \cdot (1 - r) \cdot \chi(r) dr \tag{2}$$

Therefore, the notch stress intensity factor is defined as a function of effective distance and effective stress:

$$K_\rho = \sigma_{ef} \cdot (2\pi X_{ef})^\alpha \tag{3}$$

where K_ρ, σ_{ef} and X_{ef} are the notch stress intensity factor, effective stress and effective distance, respectively, and α is the slope of the stress distribution in region III. The exponent α depends on the notch angle and is equal to $\alpha = 0.5$ if the sides of the notch are parallel.

A description of this kind of notch tip stress distribution is given in Fig. 3. The procedure to determine the effective distance with the help of the relative stress gradient is also given in this figure (see Fig. 4).

For the 1000 N fixed load and for the failure load which depends on the relative notch length, the notch stress intensity factor decreases by covering the defect with a glued composite patch. Its value decreases more with a type III patch which covers the specimen totally along its length. At constant load, the notch stress intensity factor increases by the effect of

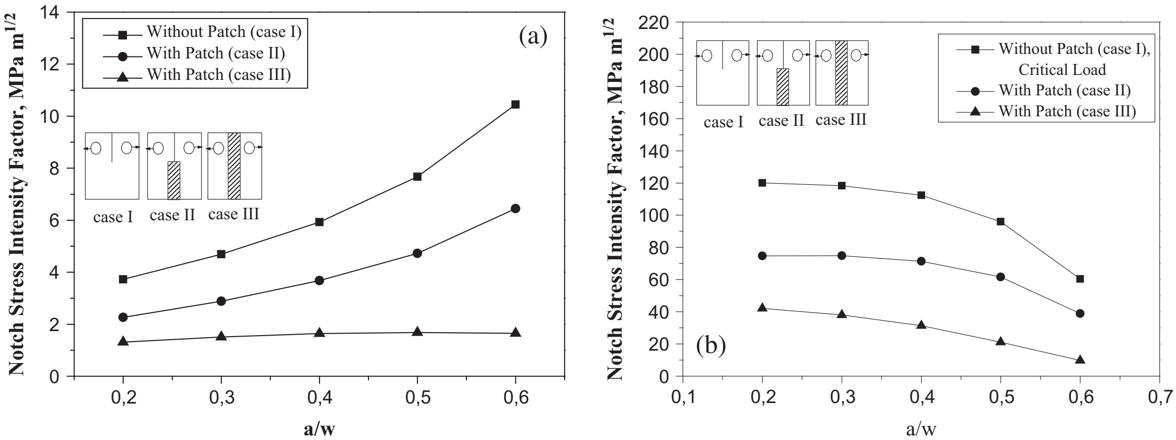

Fig. 4. Influence of relative notch depth on applied notch stress intensity factor (a) and critical notch stress intensity factor (b).

reducing the ligament with the relative notch length a/W. At failure load, the critical notch stress intensity factor considered as the notch fracture toughness decreases due mainly to the constraint effect which affects the critical load.

5. Determination of *T*-stress

T-stress is a characteristic of the defect tip stress distribution. For a crack, Larsson and Carlsson [9] have suggested describing the elastic stress field at the crack tip by three terms and introduce for the first time the *T* term as the second one of the series:

$$\sigma_{ij} = \frac{K_{ij}}{\sqrt{2\pi r}} \cdot f_{ij}(\theta) + T\delta_{li}\delta_{lj} + O(r) \tag{4}$$

Its validity is limited to the elastic part of the stress distribution. For a notch, the validity is limited for notch tip distances greater than the effective distance. For a notch with infinite acuity, Williams [10] has given a solution for elastic stress distribution as the following series:

$$\sigma_{yy} = \frac{A_1}{\sqrt{r}} + A_2 + A_3\sqrt{r} + A_4 r + A_5\sqrt{r^3} \tag{5}$$

where A_2 is equal to $T/4$. Therefore, ideally *T*-stress is a constant stress which acts along the crack direction and shifts the opening stress distribution according to the sign of this stress. For stress distribution emanating from a blunted crack or notch, *T*-stress is not constant along the ligament. This leads us to consider a conventional value defined as the effective *T*-stress.

The stress distribution ahead of a crack tip depends on the polar angle θ, as we can see in Eq. (4). However, for some particular θ angles, the *T*-stress is given by particular values of the difference between the opening stress σ_{yy} and the stress parallel to the crack σ_{xx}. Particularly for $\theta = 0$, the *T*-stress is given by:

$$T = (\sigma_{xx} - \sigma_{yy})_{\theta=0} \tag{6}$$

Eq. (6) is the basis of the so-called Stress Difference Method (SDM), which was proposed by Yang and Ravi-Chandar [7]. The stress distribution in the direction $\theta = 0$ is generally computed by the Finite Element method.

Fig. 5 shows the *T*-stress distribution along the ligament in the CT specimen with a patch (type III) (applied tensile load 1000 N). *T*-stress increases with the distance to the notch tip and stabilizes at a distance greater than 1 mm. Increases of the relative notch depth induce a loss of constraint, i.e., *T* has a higher negative value. A similar evolution to that of the unpatched specimen is noted: the *T*-stress constraint changes from a negative to a positive value and increases with increasing defect length.

6. Determination of effective *T*-stress T_{ef}

Due to the fact that *T* is not constant, the considered value is obtained by a conventional definition. The effective *T*-stress is the value of *T* at the beginning of the stabilization of the *T*-stress distribution. This distance is called the *T* effective distance $X_{ef,T}$. In order to get this value more precisely, an analytical method is used. The *T* distribution along a ligament is fitted by a polynomial function (Eq. (7)).

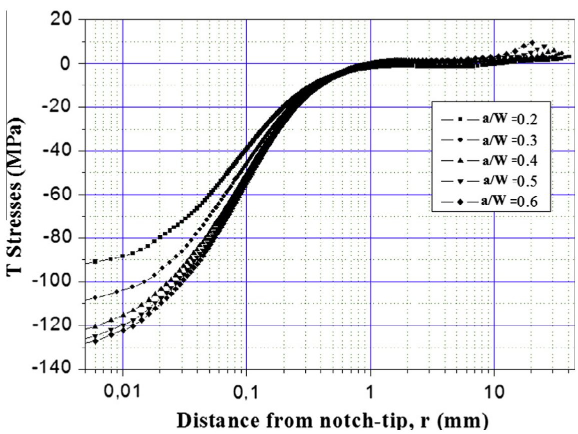

Fig. 5. *T*-stress distribution along the ligament in the CT specimen with patch (type III) (applied tensile load 1000 N).

$$T_{xx}(x) = \sum_{i=0}^{n} a_i x^i \tag{7}$$

where a_i are the coefficients and x the distance. The relative gradient of the T-stress is given by:

$$\chi(x) = \frac{1}{T_{xx}(x)} \cdot \frac{dT_{xx}(x)}{dx} \cdot \frac{\sum_{i=0}^{n} i a_i x^{i-1}}{\sum_{i=0}^{n} a_i x^i} \tag{8}$$

The weight function ϕ is written as follows:

$$\phi(x) = 1 - \frac{x \sum_{i=0}^{n} i a_i x^{i-1}}{\sum_{i=0}^{n} a_i x^i} \tag{9}$$

The T effective distance can be obtained by the Taylor approach for the vicinity of the notch tip. It corresponds to the minimum point of the relative gradient of T-stress:

$$\frac{d\chi(x)}{dx} \tag{10}$$

Substituting Eq. (9) in the relation (10), the following relationship can be obtained:

$$\frac{d\chi}{dx} = \frac{\sum_{i=0}^{n} (i^2 a_i x^{i-2} - i a_i x^{i-2})}{\sum_{i=0}^{n} a_i x^i} - \frac{\sum_{i=0}^{n} a_i x^{i-1}}{\sum_{i=0}^{n} a_i x^i} = 0 \tag{11}$$

The effective T-stress is estimated by averaging the T-stress over the T effective distance

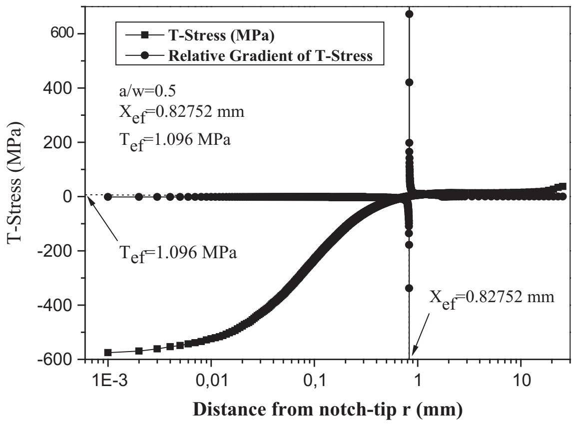

Fig. 6. Schematic diagram of the determination of the T-stress by the proposed method and the gradient of the T-stress near the notch tip and effective distance (CT specimen without patch $a/W = 0.5$ applied tensile load 1000 N).

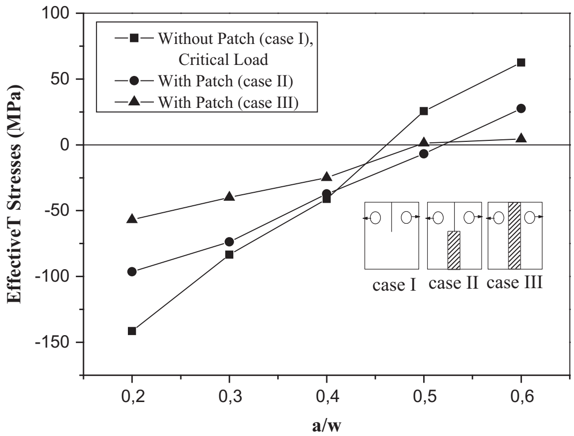

Fig. 7. Evolution of the effective T_{ef} stress with relative notch depth a/W for the three configurations and for critical loads given in Table 2.

$$T_{ef} = \frac{1}{X_{ef}} \cdot \int_0^{X_{ef}} T_{exx}(r) \cdot \Phi(r)\, dr \tag{12}$$

Here, $T = T_{xx} = (\sigma_{xx} - \sigma_{yy})_{\theta=0}$ is the T-stress distribution along the ligament (r) in the xx direction and ϕ (r) is the weight function.

Fig. 6 shows a graphic representation of the T-stress along the ligament, the gradient of this distribution and the technique of the minimum of the gradient to deduce the two parameters: the T effective distance $X_{ef,T}$ and the effective T-stress, T_{ef}.

Fig. 7 reports the evolution of the effective T_{ef} stress with relative notch depth a/W for the three configurations (with and without patch). For critical loads given in Table 2, the effective T-stress is called critical $T_{ef,c}$. This value increases with the relative notch length and corresponds to an increase of constraint. For a relative notch length $a/W \leqslant 0.5$ for the specimen with a patch and for $a/W \leqslant 0.45$ for the specimen without a patch, the value of $T_{ef,c}$ is negative. Positive values of $T_{ef,c}$ have some influence on the possibility of crack bifurcation after fracture initiation [11].

7. Patch repairing index (RPI) in the Fracture Toughness–Constraint Diagram (FTCD)

By plotting the critical notch stress intensity factor versus the critical effective T-stress $T_{ef,c}$ in the plane Notch stress intensity factor – effective T-stress [T_{ef}–Kr], one plots the Failure Material Master Curve (FMMC). This FMMC is a decreasing function of $T_{ef,c}$, i.e., fracture toughness decreases when constraint increases. We note that, in our case, the evolution of fracture toughness is non-linear.

Fig. 8 reports the evolution of the applied and critical notch stress intensity factors with relative notch depth a/W for the two types of patch. Points associated with critical notch stress intensity factors give the FMMC. One notes that the (13) of the defect decreases more with the type III patch. In the plane [T_{ef}–K_ρ], any assessment point below the FMMC represents a safe

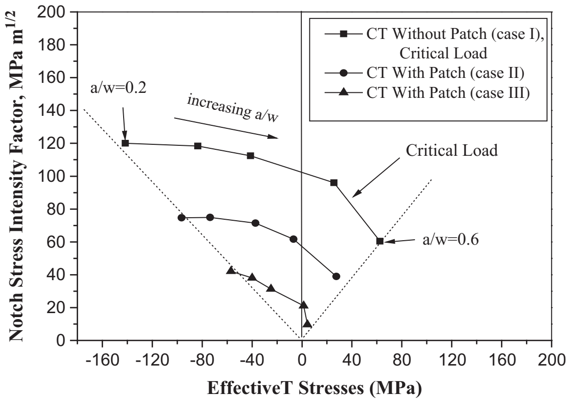

Fig. 8. Evolution of the notch stress intensity factor with relative notch depth a/W for the two types of patch and the FMMC.

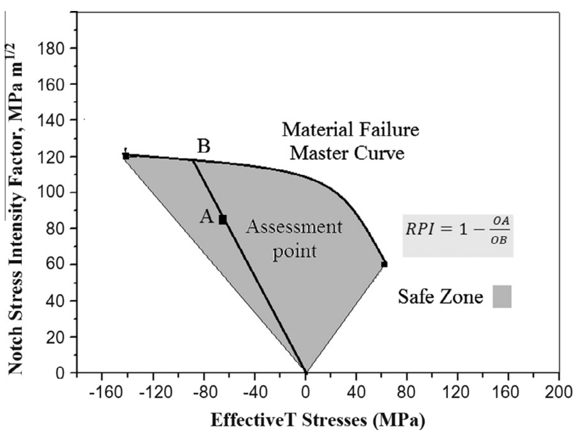

Fig. 9. Patch repairing index (RPI) in the Fracture–Constraint Diagram (FCD).

Table 3
Value of RPI with relative notch length.

a/W	0.2	0.3	0.4	0.5	0.6
RPI (%)	61.8	61.9	68.4	78.6	87.7

situation. A line from origin O and passing through any assessment point A intercepts the FMMC at point B (Fig. 9). The patch repairing index (RPI) is defined as:

$$RPI = 1 - OA/OB \tag{13}$$

This RPI is an indicator of the remaining harmfulness of a defect after repair. Values of RPI with relative notch lengths are given in Table 3.

8. Conclusion

The use of composite for repairing damaged pipe is a fast and economic method without service interruption. However, the remaining repair defect retains some harmfulness. This residual harmfulness needs to be evaluated in order to see if the security is at acceptable level. This can be done using the patch repairing index (RPI) measured by the method described in this paper. A conventional value of this admissible index is necessary. Associated with a safety factor of 2, a criterion of admissible RPI can be a value less than 50%. The length of the patch as well as the thickness of the glue layer has a major influence on the defect driving force in terms of the J integral or notch stress intensity factor, as mentioned by Ref. [12]. This will be the direction of our future work.

References

[1] 6th Report of the European gas pipeline incident data group, 1970–2004; 2005.
[2] 7th Report of European gas pipeline incident data group, 1970–2007, gas pipeline incidents, December; 2008. p. 1–33 <http://www.EGIG.nl>.
[3] Chow WT, Atluri SN. Composite patch repairs of metal structures: adhesive nonlinearity, thermal cycling, and debonding. AIAA J 1997;35(9):1528–35.
[4] Jones R, Chiu WK. Composite repairs to crack in metallic components. Comp Struct 1999;62:431–43.
[5] Fazzini PG, Otegui JL. Influence of old rectangular repair patches on the burst pressure of a gas pipeline. Int J Pressure Vessels Piping 2006;83:27–34.
[6] Pluvinage G. Notch effects in fatigue and Fracture. Editor Kluwer; 2001, ISBN 1-4020-1609-3.
[7] Yang B, Ravi-Chandar K. Evaluation of elastic T-stress by the stress difference method. Eng Fract Mech 1999;64:589–605.
[8] Hadj Meliani M, Azari Z, Pluvinage G, Matvienko YuG. The effective T-stress estimation and crack paths emanating from U-notches. Eng Fracture Mech 2010;77(11):1682–92.
[9] Larsson SG, Carlsson AJ. Influence of non-singular stress terms and specimen geometry on small-scale yielding at crack tips in elastic–plastic materials. J Mech Phys Solids 1973;1(21):263–77.
[10] Williams ML. Stress singularity resulting from various boundary conditions in angular corners of plates in extension. J Appl Mech 1952;19(4):526–8.
[11] Pluvinage G, Capelle J, Hadj Méliani M. A review of fracture toughness transferability with constraint and stress gradient. To Appear in Fatigue and Fracture of Engineering Material and structure, 2014.
[12] Jodin P. Fracture mechanics analysis of repairing a cracked pressure pipe with a composite sleeve in safety reliability and risks associated with water oil and gas pipelines. In: Pluvinage G, Elwany MH, editors. Springer; 2008. ISBN 978-1-4020-6524-8.